

Knowledge-based Segmentation of Calvarial Tumors in Computed Tomography Images

Aleksandra Popovic¹, Martin Engelhardt² and Klaus Radermacher¹

¹Chair of Medical Engineering, Helmholtz-Institute for Biomedical Engineering,
RWTH Aachen University

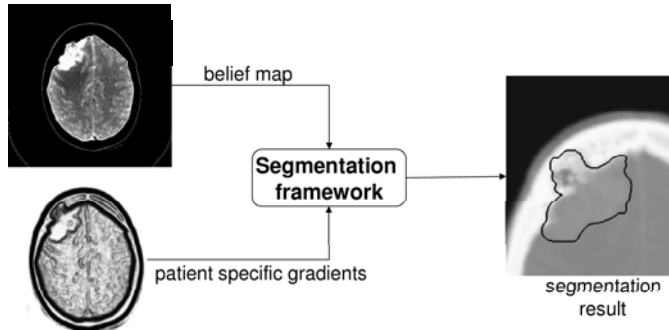
²Clinic for Neurosurgery, Ruhr-University Bochum
Email: popovic@hia.rwth-aachen.de

Abstract. This paper presents an image segmentation algorithm based on the level sets deformable model framework, guided with patient specific information as well as *a priori* knowledge gained from the training set. The driving application is segmentation of 3D calvarial tumors from Computed Tomography images, which is a challenging task considering the fact that they reside both in calcified and soft tissue, have ill-defined borders, and occupy wide range of image intensities. Level set algorithms are widely used for complex segmentation problems since they show good robustness in presence of inhomogeneities and noise. However, for segmentation of object with fuzzy borders, standardly used surface evolution forces based on the gradients often fail to reach the convergence. We present an algorithm that combines image specific information and *a priori* knowledge on image intensities of objects under investigation. The knowledge modeling framework is presented, followed by the segmentation algorithm, and the validation of the results.

1 Introduction

The CRANIO project for computer and robot assisted craniotomy [1] tackles the problem of efficient and effective removal of calvarial tumors, including operation planning and surgery. Within this framework a need for automatic and semi-automatic delineation of calvarial tumors emerged.

Calvarial tumors can be found anywhere from the meninges to the area under the skin of the head. The variety of origin and location of calvarial tumors results in diverseness in their appearance in Computed Tomography (CT) images. They are standardly located in both soft and calcified tissue, occupying a large range of image intensities. Furthermore, local calcifications and ossifications, which are both very common in those lesions, represent persistent problem since they introduce large discontinuities. Thus, region or edge based algorithms often fail to properly segment the entire tumor. In our previous study [2] we have demonstrated that in comparison with other segmentation methods, level set framework showed the most promising results. This is due to its capability to advance in two or more fronts and finally merge together into one bounding surface, which is the key feature when an object with different tissue types is to

Fig. 1. Flowchart of the segmentation process.

be segmented. In this paper, we propose an extension to the approach presented in our previous work [2], adding a knowledge-based propagation term to the segmentation framework.

The most common approach in modeling of *a priori* knowledge in medical image segmentation is to define an *a priori* shape and adjust it to the borders of the specific object to be segmented. Although this method has been successful in segmentation of healthy anatomy [3], Clark et al. point out that prior shapes are virtually unfeasible for segmentation of tumors, due to the morphological discrepancy between the subjects [4].

2 Methods

The segmentation approach proposed here relies on the level sets based deformable model, guided with gradients derived from the image under subject and the individual belief map generated from the training set (Fig. 1). A belief map indicates a likelihood that an image element belongs to the tumor. In this work, belief map is solely based on the grey-levels of the image.

2.1 Belief Map Generation

Let \mathcal{T} be a training set of grey-level images of tumor extracted region, $T_i(\mathbf{x})$, $T_i : \mathbb{R}^3 \rightarrow \mathbb{R}$, $i = 0 \dots n_t - 1$, $\mathbf{x} = [x, y, z]^T$. It is important to notice that each image from the training set, T_i , contains grey-levels of the tumor while all other parts of the image are set to zero. Tumors were previously manually segmented by an expert. For each image in \mathcal{T} a maximum likelihood estimation of a Gaussian distribution of the grey-levels within the tumor is computed (μ_i , σ_i). Mean Gaussian distribution is found at:

$$\bar{\mu} = \frac{1}{n_t} \sum_{i=0}^{n_t-1} \mu_i, \quad \bar{\sigma} = \frac{1}{n_t} \sum_{i=0}^{n_t-1} \sigma_i. \quad (1)$$

Let $I(\mathbf{x})$ ($I: \mathbb{R}^3 \rightarrow \mathbb{R}$) be an image to be segmented. In each image element, i.e. voxel, a likelihood that given voxel belongs to the tumor is defined as:

$$B(\mathbf{x}) = \frac{1}{\sigma\sqrt{2\pi}} e^{-\frac{I(\mathbf{x})-\mu}{2\sigma^2}} \quad (2)$$

2.2 Level Set Evolution

Level sets are generalized surface movement framework [5], where surface evolution is defined as:

$$\frac{\partial\Psi(\mathbf{x}, t)}{\partial t} = -\nabla\Psi(\mathbf{x}, t) \cdot F(\mathbf{x}), \quad (3)$$

$\Psi(\mathbf{x}, t)$ is a hypersurface defined on the entire image while the surface under subject is a zero level set of Ψ . Speed function, $F(\mathbf{x})$, defines velocity and direction of movement in each point of the front. In our previous work [2], we have used following speed function:

$$F(\mathbf{x}) = F_p(\mathbf{x}) + F_c(\mathbf{x}) + F_a(\mathbf{x}), \quad (4)$$

$$F_p = \alpha \cdot g_I(\mathbf{x}), \quad F_c = -\beta \cdot g_I(\mathbf{x}) \cdot k(\mathbf{x}), \quad F_a = \gamma \cdot \nabla Q(\mathbf{x}), \quad (5)$$

where k is the curvature of the current front ($\nabla \frac{\nabla\phi}{|\nabla\phi|}$), g_I is an edge potential map, and Q is the advection force, defined as:

$$g_I(\mathbf{x}) = \frac{1}{1 + |\nabla G_\sigma * I(\mathbf{x})|}, \quad Q(\mathbf{x}) = -|\nabla(G_\sigma * I(\mathbf{x}))|, \quad (6)$$

where G_σ is the Gaussian filter. F_p , F_c , F_a are propagation, curvature, and advection speed terms, respectively. This terms are weighted using three constants $[\alpha, \beta, \gamma]$.

Herein, we propose an extension to this framework by introducing additional term $B(\mathbf{x})$, Eq. 2, into the propagation part of the speed function:

$$F_p(\mathbf{x}) = \alpha \cdot (\delta \cdot B(\mathbf{x}) + g_I(\mathbf{x})). \quad (7)$$

The level set propagation is realized within the National Library of Medicine Image Segmentation and Registration Toolkit (<http://www.itk.org>).

2.3 Validation of the Segmentation Results

Statistical metrics for validation of a segmentation outcome in comparison with the ground truth used in this study are defined as follows:

$$DSC = \frac{2 \cdot TP}{2 \cdot TP + FP + FN}, \quad (8)$$

$$sensitivity = \frac{TP}{TP + FN}, \quad specificity = \frac{TN}{TN + FP}, \quad (9)$$

where TP, FP, TN, FN, are number of true positives, false positives, true negatives, and false negatives, respectively. Dice Similarity Coefficient (DSC) is a special case of the kappa statistics for very large samples.

Table 1. Minimal and maximal value of three validation metrics for five patient

Patient	Diagnosis	Sensitivity	Specificity	DSC
A	Metastasis	0.59÷0.77	0.96÷0.96	0.68÷0.70
B	Meningioma (WHO II)	0.83÷0.90	0.98÷0.99	0.72÷0.86
C	Meningioma (WHO III)	0.81÷0.88	0.98÷0.99	0.79÷0.83
D	Meningioma (WHO I)	0.81÷0.97	0.95÷0.99	0.81÷0.89
E	Meningioma (WHO I)	0.90÷0.96	0.98÷0.99	0.84÷0.88

3 Materials

Five patient datasets were used, four thereof with diagnosed meningioma and one with skull metastasis. All patients were scanned with Siemens Somatom Plus CT, resolution 0.43x0.43x3mm. Tumors were manually delineated by one of the coauthors (M.E.). For each test a group of four datasets is used for the knowledge modeling and fifth dataset for the validation of segmentation results.

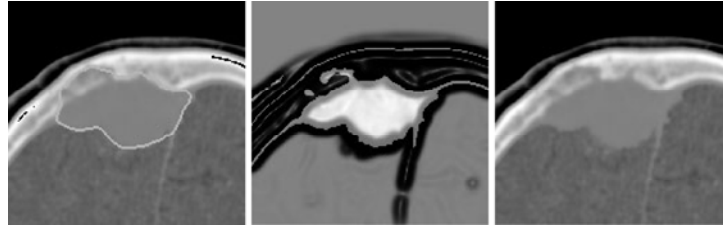
4 Results

In the Table 1 validation results for the five datasets under subject are shown. Different results are archived by varying algorithm parameters $[\alpha, \beta, \gamma, \delta]$. For all patients, a significant improvement compared to classical level sets algorithm [2] for all three validation metrics is noticeable. Figure 2 presents an example of the segmentation workflow and a segmentation result. Entire segmentation process lasts approximately one minute.

5 Discussion and Conclusion

For all patients, a significant improvement compared to classical level sets algorithm [2] in all three validation metrics is noticeable. The algorithm here presented uses topological flexibility of level sets (e.g. fronts merging) together with a knowledge-based term which stabilizes the algorithm and improves accuracy. As Zijdenbos et al. [6] specified, DSC of more then 0.7 is considered to be a very good segmentation result. In this study, for four patients, it was possible to reach DSC of more then 0.8, with the sensitivity of above 0.85. However, segmentation results for patient 'A' are significantly less accurate, due to the fact that this patient was diagnosed with a very large metastasis expanding to extra calvarial soft tissue. It is clear from the Table 1 that segmentation accuracy decreases with severity of the tumor (WHO grade). In our future work, we will focus on improvements of knowledge modeling. First tests using a discrete method as in Touhami et al. [7] showed promising results.

Fig. 2. From left to right: Original image, represented using two sided intensity window, Speed function, and a segmentation result.



Acknowledgement. This project is funded in part by the German Research Foundation (DFG), Framework 'Surgical Navigation and Robotics' (DFG RA548/2-1)

References

1. Popovic A, Engelhardt M, Wu T, Porthene F, Schmieder K, Radermacher K. CRANIO – Computer Assisted Planning for Navigation and Robot-assisted Surgery on the Skull. In: Lemke HU, et al, editors. Procs CARS. vol. 1256 of International Congress Series. Elsevier; 2003. p. 1269–1276.
2. Popovic A, Engelhardt M, Radermacher K. Segmentation of Skull-infiltrated Tumors Using ITK: Methods and Validation. In: ISC/NA-MIC/MICCAI Workshop on Open-Source Software at MICCAI 2005. Available: <http://hdl.handle.net/1926/21>; 2005.
3. Paragios N. A Level Set Approach for Shape-driven Segmentation and Tracking of the Left Ventricle. *IEEE Transactions on Medical Imaging* 2003;22(6):773–776.
4. Clark MC, Hall LO, Goldgof DB, Velthuizen R, Murtagh FR, Silbiger MS. Automatic Tumor Segmentation Using Knowledge-Based Techniques. *IEEE Transactions on Medical Imaging* 1998;17(2):187–201.
5. Sethian JA. *Level Set Methods and Fast Marching Methods*. vol. 3. 2nd ed. Cambridge University Press; 1996.
6. Zijdenbos AP, Dawant BM, Margolin RA, Palmer AC. Morphometric Analysis of White Matter Lesions in MR Images: Method and Validation. *IEEE Transactions on Medical Imaging* 1994;13(4):716–724.
7. Touhami W, Boukerroui D, Cocquerez JP. Fully Automatic Kidneys Detection in 2D CT Images: A Statistical Approach. In: Duncan J, Gerig G, editors. Eighth International Conference on Medical Image Computing and Computer-Assisted Intervention (MICCAI). vol. 3749 of Lecture Notes on Computer Science. Springer-Verlag; 2005. p. 262–270.